Photocurrent Response Characteristics of ZnO/TiO₂ Nano Thin Films on Si/SiO₂ Substrate Using Sol-Gel Method

Ahmed A. Auda[1, *], Hikmat A. J. Banimuslem[2], Burak Y. Kadem[3]

[1]Department of Physics, College of Science, University of Babylon, Babylon, IRAQ
[2]Department of Physics, College of Science, University of Babylon, Babylon, IRAQ
[3]Department of Physics, College of Science, Al-Karkh University of Science, Baghdad, IRAQ

ARTICLE INFO

ABSTRACT

The Sol-Gel method synthesizes ZnO/TiO2 thin film structures on Si/SiO2 substrates, particularly enhancing photocurrent response and photovoltaic characteristics. Using the Sol-Gel method, the study aims to provide insights into the features and implications of the photocurrent response under visible light illumination. Examining various parameters such as current amplitude, resistivity, rise time, fall time, rise time to fall time ratio, and photocurrent amplitude to rise time/fall time ratio, this research seeks to understand the performance of the synthesized thin film structures. Among the studied delicate film structures, the hybrid ZnO: TiO₂ exhibits the highest current responsiveness, while TiO₂ and TiO₂/ZnO demonstrate dark everyday phenomena. These findings hold significance for optimizing the design of photovoltaic devices utilizing the Sol-Gel method. By investigating ZnO/TiO₂ thin film structures on Si/SiO₂ substrates using the Sol-Gel method, this research provides valuable insights into these structures' performance and potential applications in photovoltaics. The results contribute to advancing renewable energy technologies and guide the development of efficient photovoltaic devices.

1.Introduction

Photocurrent devices, essential for converting light into electrical current, are considered significant in light-to-energy conversion processes. Among the various photocurrent technologies, thin film structures have been recognized as attractive options for achieving high-performance and cost-effective solutions [1]. Remarkably, thin films like titanium dioxide (TiO₂) and zinc oxide (ZnO) have gained value due to their lightweight, cost-effectiveness, and uses in multiple applications [2,3]. Furthermore, heterojunctions like ZnO/TiO₂ have shown a good chance of enhancing photo-conversion efficiency [4]. In addition, studying the thin films' time-dependent properties will lead to a possible advancement of photocurrent devices. The sol-gel method, a widely recognized technique for fabricating thin film structures, allows for meticulous control over material synthesis, enabling the deposition of homogeneous and controlled films [5,6,7]. This versatile approach permits the customization of thin film composition and morphology, creating high-quality interfaces between layers and improved coating performance [8]. Tailoring the properties of thin films to meet specific application requirements is achievable by optimizing key parameters, such as substrate temperature and solution concentration [9]. Moreover, precise control over film thickness is vital for accuracy optics applications, where photocurrent responsiveness significantly influences the efficiency of light-to-electrical conversion [10]. The electrical conductivity of thin film structures is notably influenced by their resistivity, facilitating efficient charge movement and minimizing energy losses [11]. Additionally, understanding the time-dependent variables of

---
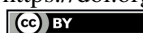
photocurrent response, namely rise time (R.T.) and fall time (F.T.), provides crucial insights into the performance and stability of thin film structures [12]. The R.T./F.T. ratio leads to information about the decay behavior of photocurrent and the potential persistence of current after light removal, providing essential information on charge recombination and carrier dynamics within the material [13]. Furthermore, the photocurrent amplitude to rise time/fall time ratio I/(R.T./F.T.) ratio measures current response efficiency, considering both the rise and fall times and hints at potential improvements in device performance [14]. Notably, negative-current phenomena have been observed in TiO_2 and TiO_2/ZnO thin film structures when the light is off. The presence of trap states within these materials can lead to electron flow in the opposite direction, and understanding these phenomena is essential for reducing energy losses and enhancing overall performance [15]. Understanding the behavior and properties of these thin film materials allows for enhancing their design, synthesis processes, and combination into efficient photocurrent response structures. The Si/SiO_2 substrate also provides a robust foundation for a thin film with highly favorable properties for enhancing photocurrent response [16]. The stable interface offered by the Si/SiO_2 substrate ensures good adhesion and minimal defects, further improving photocurrent response and overall device efficiency [17]. Understanding characteristics and behavior in these thin film structures is critical to optimizing photocurrent response and harnessing their potential in next-generation photocurrent response devices [18].

2. Materials and Methods

The synthesis method of the thin films is sol-gel. The ZnO and TiO_2 were prepared according to these steps: 6.645g of zinc acetate dihydrate (Zn $(CH_3COO)_2 \cdot 2H_2O$) was slowly added to 40ml of 2-methoxyethanol ($CH_3OCH_2CH_2OH$) under stirring on a hotplate stirrer at $60\pm5^{o}C$ to achieve a molar concentration of 0.3 M. To the resulting solution, 10 ml of monoethanolamine (MEA) ($HOCH_2CH_2NH_2$) was added dropwise as a stabilizer, and the answer was stirred for 30 minutes. The solution was left by adding hydrochloric acid (HCl) dropwise for acceleration for an additional 60 minutes. The answer was then aged for 24 hours before deposition. The TiO_2 solution was made by adding 3.23 ml of titanium tetraisopropoxide Ti $\{OCH(CH\square)\ \square\}\ \square$ to 40 ml of 2-methoxyethanol at $60\pm5^{o}C$ with a molar concentration of 0.3 M. Ten sprays were spread out over one minute to remove moisture between each layer. The resulting films were aged 24 hours before undergoing a 30-minute annealing process. The ZnO and TiO_2 thin films were annealed at $380^{o}C$ and $600^{o}C$, respectively. To synthesize hybrid (ZnO: TiO_2) heterostructure, the ZnO and TiO_2 solutions were composited in a 1:1 ratio under stirring for 30 minutes before ageing for 24 hours. After deposition, the annealing process was performed for 30 minutes at $380^{o}C$. For making the bilayer (TiO_2/ZnO) heterostructure, the annealing process was executed at $380^{o}C$ for the ZnO layer and $600^{o}C$ for the TiO_2 layer. Photocurrent devices were made by depositing ZnO, TiO_2, ZnO: TiO_2, and TiO_2/ZnO solutions on clean Si/SiO_2 substrates. All the answers of thin films were deposited using a spray pyrolysis method on a hotplate set at $150^{o}C$. The resulting samples were coated with aluminum (Al) electrodes on the sides, and the produced device is shown in Fig 1.
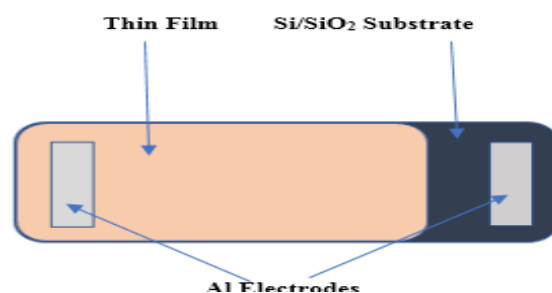

Fig. 1. Top view of the photocurrent response device.

3. Results and Discussion

3.1. Structural properties

The structural properties of the studied thin films of ZnO, TiO_2, ZnO:TiO_2 heterostructures (hybrid) and ZnO/TiO_2 (layer) was carried out using XRD pattern;

results are shown in Fig.2. The diffraction peaks of ZnO labeled at 2θ of 32.047^{o} (100), 34.3493^{o} (002), 36.3712^{o} (101), and 56.7618^{o} (110) are fitted well with the hexagonal ZnO wurtzite structure (reference code: 01-079-0205)
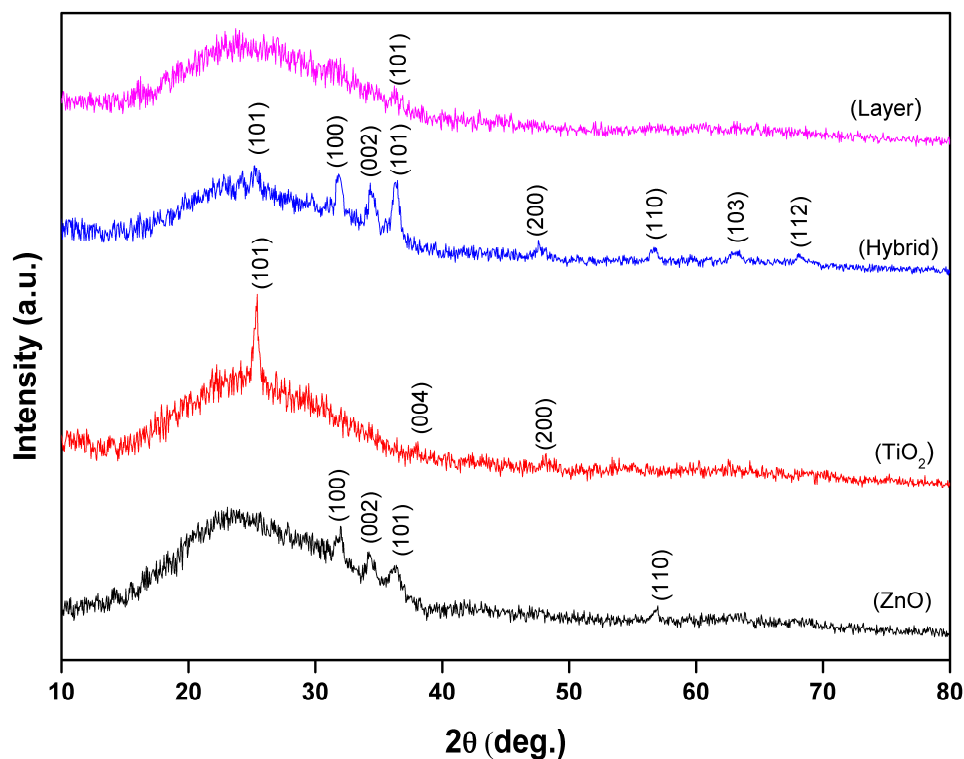
.

Fig. 2. XRD pattern of the four thin film structures.

On the other hand, TiO_2 has exhibited three peaks at 2θ of 25.395^o (101), 37.821^o (004), and 48.073^o (200) which are matched with Reference code: 00-001-0562 Anatase The crystallite size (D) was calculated using the Scherer equation as follows:

$$D = \frac{k\lambda}{\beta cos\theta} \qquad (1)$$

where θ is Bragg angle, λ is the incident X-ray wavelength (0.15406 nm), (k) is a dimensionless shape factor, with a value close to unity (0.9) and β is the full-width at half maximum (FWHM) of the diffraction peak.

The crystallite size (D) of ZnO is ranged from 12.3-21.4 nm, while, TiO_2 has shown crystallite size (D) of 12.3-14.0 nm. After making hybrids, crystallite size (D) has reduced to be in the range of 9.7-17.3nm. Also, the bilayer structure exhibited small crystallite size (8.8nm). The eight peaks of hybrid heterostructure are all matched with reference code: 01-076-0704, hexagonal ZnO structure only the peaks at 25.28^o , 47.76^o, and 63.12^o are matched with reference code: 00-001-0562. The layer heterostructure XRD pattern shows only one peak at position 36.203^o that matched with Reference. code: 01-076-0704 ZnO, and Reference code: 00-029-1361 Hongquiite TiO_2. This peak intensity is more matched with Reference code: 01-076-0704 ZnO, so this mean that the ZnO layer is more effective than that of TiO_2, all matched peaks are listed in table 1 (a), and (b).

Table 1(a); Scherer calculation of matched peaks for pure ZnO, and TiO_2 .

Thin Film	FWHM [°2θ]	Peak pos. [°2 θ]	D [nm]
ZnO	0.394	32.047	21.4
	0.590	34.349	14.3
	0.689	36.371	12.3
	0.720	56.762	12.7
TiO_2	0.590	25.394	14.0

| 0.689 | 37.821 | 12.3 |
| 0.720 | 48.073 | 12.2 |

Table 1(b);Scherer calculation of matched peaks for heterostructures $ZnO:TiO_2$, and TiO_2/ZnO.

Thin Film	FWHM [°2θ]	Peak pos. [°2 θ]	D [nm]
ZnO :TiO$_2$	0.850	25.280	9.7
	0.492	31.834	17.1
	0.492	34.412	17.2
	0.492	36.345	17.3
	0.787	47.765	11.2
	0.590	56.695	15.5
	0.960	63.121	9.8
	0.900	68.125	10.8
ZnO/ TiO$_2$	0.960	36.203	8.8

3.2.Morphological properties

The morphological properties were investigated using scanning electron microscope (SEM) technique. SEM images shown in Fig.3 revealed that ZnO (a) has exhibited more spherical like shapes while TiO_2 (b), has demonstrated nanoribbon like shapes with homeotropic alignment.
Hybrid ($ZnO:TiO_2$) thin film structure image demonstrates the overlap between two structures of ZnO

and TiO_2, as opposed to the layer structure, which appears as two layers. It could be said that the synthesis process and annealing temperature has resulted in changing the shape of the thin films particles; the bulk sizes of the ZnO are (44-166 nm), TiO_2 are (28-48 nm), hybrid (c), are (67-221 nm), and finally layer (ZnO/TiO_2) (d), structure are (139-267nm). These sizes do not actually correspond to nanoparticles (NPs); rather, they describe a collection of several NPs that came together to form the NPs aggregations.
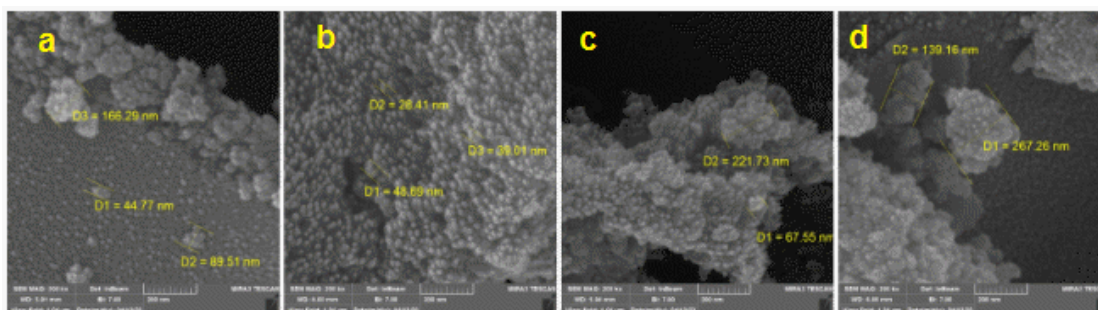

Fig. 3. SEM images for all thin film structures synthesised by sol-gel ZnO (a), TiO_2 (b), $ZnO:TiO_2$ (hybrid) (c), and TiO_2/ZnO (bilayer)

The structural and morphological analysis from XRD and SEM proved that the thin films under investigation, including ZnO, TiO_2, ZnO: TiO_2 hybrid structures, and TiO_2/ZnO bilayer structures, have nano-sized characteristics. The sizes of the crystallites and bulk frames were within the nano-scale range. These results were conducted by Auda et al. [19].
3.3. I-V Characteristics
The I-V behavior of the thin film structures demonstrates distinct characteristics in the forward bias region, as shown in Fig 4. Under light illumination, the

resistance of all forms decreases, resulting in a higher current flow. This behavior is desirable for efficient charge extraction and transport in photovoltaic devices. However, all structures align with the x-axis in the reverse bias region, indicating a limited current flow [20]. The resistance values measured at the ohmic behavior (0-1 volt) provide insights into the conductivity of the thin film structures. Among the individual films, TiO_2 exhibits a resistance of 2.79×10^5 Ω at light OFF, which decreases to 1.90×10^5 Ω at dawn ON, resulting in a RON/ROFF ratio of 0.68. ZnO

demonstrates lower resistance values, with 1.65×10^5 Ω at light OFF and 1.37×10^5 Ω at light ON, corresponding to a RON/ROFF ratio of 0.83. The ZnO: TiO$_2$ hybrid structure exhibits a relatively higher resistance, with 8.38×10^5 Ω at light OFF and 1.60×10^5 Ω at light ON. This significant decrease in resistance leads to a meagre RON/ROFF ratio of 0.19, indicating an efficient utilization of the generated photocurrent. On the other hand, the TiO2/ZnO bilayer heterostructure has a resistance of 3.46106 at light OFF and 1.70106 at light ON, resulting in a RON/ROFF ratio of 0.49. The observed resistance characteristics suggest that the conductivity of the thin film structures improves under light illumination. The decrease in resistance can be attributed to enhancing charge carrier generation, transport, and collection. The variations in resistance

values among the structures highlight the importance of material composition and structure design in determining their conductivity and photo response [21]. The I-V behavior and resistance characteristics of TiO$_2$, ZnO, ZnO: TiO$_2$, and TiO$_2$/ZnO thin film structures for photocurrent applications (table 2)[22]. The forward bias behavior shows increased current flow under light illumination, indicating improved conductivity [23]. The facilities in the reverse bias region align with the x-axis, meaning limited current flow [24]. The measured resistance values indicate that all structures exhibit decreased resistance under light illumination [25]. Among the facilities, the ZnO: TiO$_2$ hybrid shows the most significant decrease in resistance, indicating a highly efficient photoconductive response [27].
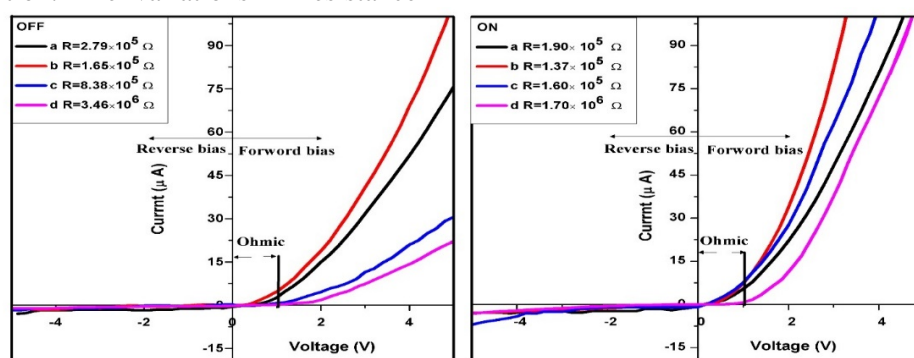

Fig. 4. I-V Characteristics of Four Thin Film Structures a) TiO$_2$, b) ZnO, c) ZnO: TiO$_2$, and d) TiO$_2$/ZnO.

Table 2. I-V Characteristics

Thin Film Structure	Resistance(Ω) Light OFF	Resistance(Ω) Light ON	R_{ON}/R_{OFF}
TiO$_2$	2.79×10^5	1.90×10^5	0.68
ZnO	1.65×10^5	1.37×10^5	0.83
ZnO: TiO$_2$	8.38×10^5	1.60×10^5	0.19
TiO$_2$/ZnO	3.46×10^6	1.70×10^6	0.49

3.4 Photocurrent response

There are two parts to this study, the first part when the source voltage is 1 volt and the second one when the source voltage is 0 volt. In both regions, the time-

dependent variables were studied to know the change in the behavior of the thin films when exposed to visible light under an 80-watt lamp
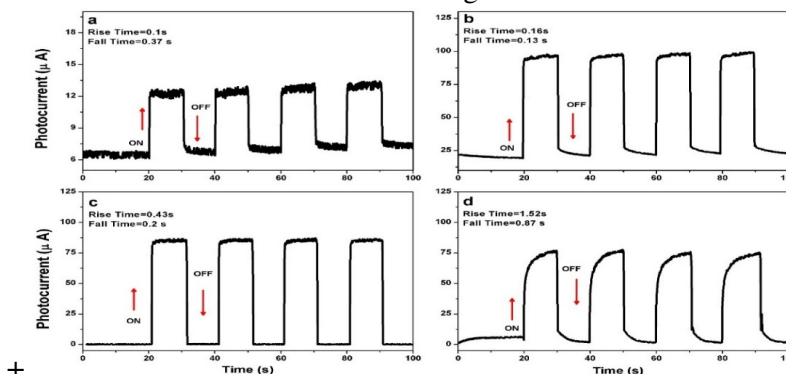

Fig 5. Behavior of photocurrent versus time at 1-volt.

The results obtained from Fig 5 show that the photogenerated current is uniform for all thin films, noting that the highest current capacity is for the hybrid structure (ZnO: TiO$_2$) and the lowest is for the system (TiO$_2$), then successively (ZnO) and approximately multi-layered (TiO$_2$/ZnO). This means that when comparing the two pure structures, the transmission of electrons between the valence band and the conduction band, representing the current generation, is higher for ZnO than for TiO$_2$.

Table 3. Dataset of photocurrent response behavior at 1V.

Thin Film Structure	R.T. (s)	F.T. (s)	R.T./F.T.	Current amplitude (μA)	I/(R/F) (μA)	Starting point (μA)	Resistivity ($\Omega.cm$)
TiO$_2$	0.1	0.37	0.27	5.87	21.72	6.48	2.37×10^4
ZnO	0.16	0.13	1.23	75.51	61.35	22.02	1.99×10^3
ZnO: TiO$_2$	0.43	0.2	2.15	85.35	39.7	0.5	1.41×10^3
TiO$_2$/ZnO	1.52	0.87	1.75	74.39	42.58	6	1.40×10^3

The average nanoparticle sizes of ZnO (15 nm) and TiO$_2$ (12 nm) obtained from Scherrer's equation and XRD results [19] offer valuable information. It can be suggested that when nanoparticles are smaller, the increased cohesion between them due to confinement effects restricts particle movement, limiting the transition from the valence band to the conduction band. Consequently, this restriction causes a decrease in the amount of photocurrent generated in the thin film structures. Understanding the relationship between nanoparticle size and photocurrent response is crucial for optimizing the performance of photocurrent devices based on ZnO and TiO$_2$ thin films. In addition, through the energy gap values [17], the energy gap for ZnO is 3.26 nm, while for TiO$_2$, it is 3.77 nm. Therefore, it can be suggested that the relatively large amount of energy gap compared to ZnO, besides the size of the nanoparticles, leads to a less photocurrent response than it is for the rest of the thin films elsewhere [27]. As for the two heterogeneous structures, it is possible to explain the behavior of the photocurrent in them about the composition effect equation [26-27]. When performing the calculations based on the above equation, the result is 2.1 for ZnO: TiO$_2$ and 1.6 for TiO$_2$/ZnO, which may increase the charge separation presiding and carrier lifetime. These results could explain the behavior of the photocurrent in the four thin films. In addition, it can be noted that the behavior characteristics are at -0 volts, in that it has the most significant current capacity and the lowest current capacity. On the other hand, it is clear from Fig 6 and Table 4 that the four thin films, under illumination by visible light, can generate photocurrent, allowing them to be applicable in devices that depend on the photocurrent generated.
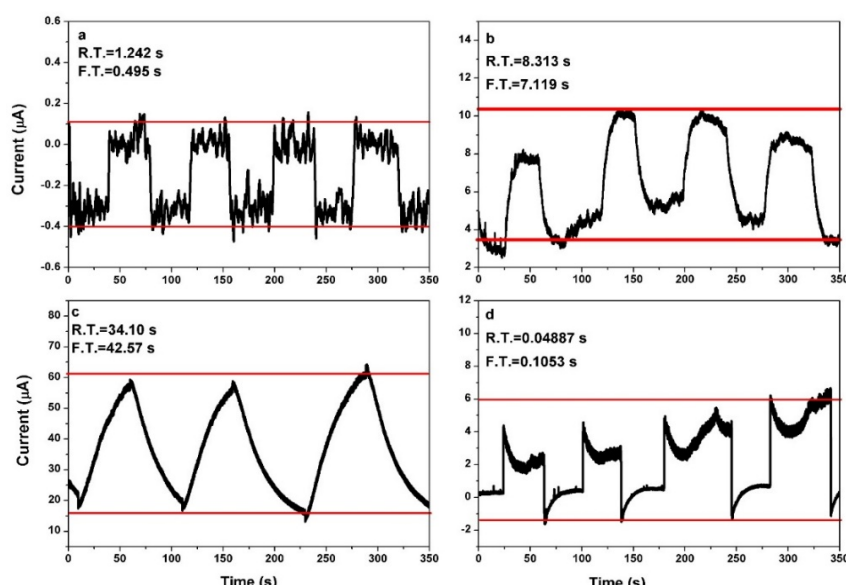

Fig 6. The behavior of photocurrent versus time at 0-volt.

The noticed dI/dt values in Figs 7,8, and Table 5 offer valuable insights into the photocurrent response of the ZnO/TiO$_2$ nanostructured thin film on the Si/SiO$_2$ substrate. The ZnO and ZnO: TiO$_2$ structures have significantly higher average dI/dt values than TiO$_2$ and TiO$_2$/ZnO, indicating enhanced photocurrent response to visible light—a more efficient charge carrier generation and transport mechanism within the ZnO-based structures.

Table 4. Dataset of photocurrent response behavior at 0V.

Thin Film Structure	R.T. (s)	F.T. (s)	R.T./F.T.	Current amplitude (μA)	I/ (R/F) (μA)	Starting point (μA)	Resistivity (Ω cm)
TiO$_2$	1.24	0.5	2.51	0.51	0.2	0.09	8.03×10^7
ZnO	8.31	7.12	1.17	6.969	5.97	4.56	3.96×10^5
ZnO: TiO$_2$	34.1	42.57	0.8	45.827	57.21	-9.28	2.55×10^4
TiO$_2$/ZnO	0.05	0.11	0.46	6.644	14.32	0.32	8.83×10^4

On the other hand, the TiO$_2$ and TiO$_2$/ZnO structures display lower average dI/dt values, indicating relatively slower photocurrent response and less efficient charge carrier dynamics. The positive average dI/dt values in the ON state demonstrate the photoconductive nature of the thin film structures, indicating an increasing photocurrent over time when exposed to visible light. Conversely, the negative average dI/dt values in the OFF state suggest a decrease in photocurrent when the light source is turned off. This implies partial recombination of charge carriers and dark current phenomena.
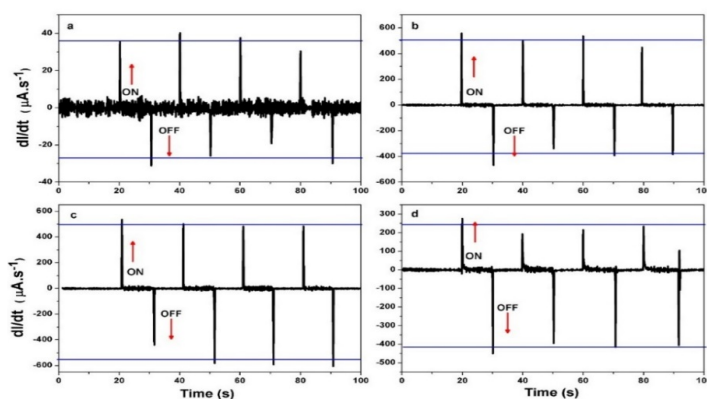

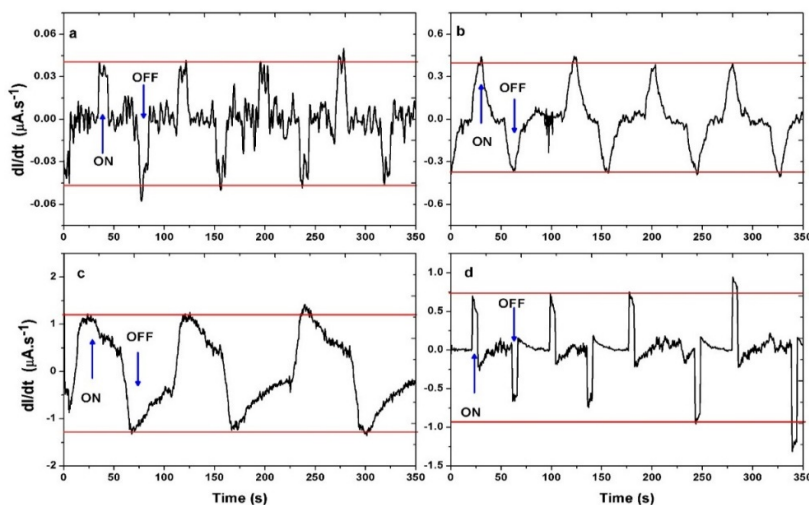**Fig 7.** The time rate of photocurrent response at 1 volt.

Fig 8. The time rate of photocurrent response at 0-volt.

The observed differences in dI/dt values between the ON and OFF states emphasize the dependence of photocurrent response on the presence or absence of visible light. These results highlight the significance of dI/dt behavior in understanding the dynamic behavior of thin film structures and their photo-response characteristics.

Table 5. The time rate of current at 1-V and 0-V.

Thin Film Structure	dI/dt (1-Volt) (μ A/s)		dI/dt (0-Volt) (μ A/s)	
	ON state	OFF state	ON state	OFF state
TiO_2	35.7	-27.3	0.04	-0.046
ZnO	506.2	-374.9	0.4	-0.37
$ZnO: TiO_2$	469.3	-551.4	1.198	-1.28
TiO_2/ZnO	243.6	-415.8	0.736	-0.92

4. Conclusions

The photocurrent response behavior of different thin-film structures was explored in this study under varying voltage conditions, employing the sol-gel method. Many significant results were obtained from the analysis of the gathered data. Firstly, variations in response speed among different structures were observed through the rise and fall times of the photocurrent. ZnO exhibited the fastest response, while TiO_2/ZnO demonstrated the shortest rise and fall times at both 1-volt and 0-volt voltage sources. Insights into the magnitude of the photocurrent generated by each structure were obtained through the current amplitudes. ZnO consistently displayed the highest current amplitude, indicating superior efficiency in converting light into a current. Efficient conversion of sunlight into current by ZnO: TiO_2 was highlighted by the I/(R/F) values, which represent the normalized photocurrent considering the ratio of rise time to fall time. Furthermore, the impact of applied voltage on the photocurrent response was shown by comparing the 1-volt and 0-volt voltage sources. ZnO exhibited the highest rate of increase at 1 volt, while ZnO: TiO_2 showed the highest rate of decrease in the OFF state, suggesting differences in response dynamics and charge carrier efficiency.

Acknowledgements:

Conflict of interests

The authors declare that they have no conflicts of interest.

References

[1] Z. Lu, H. Zhou, C. Ye, S. Chen, J. Ning, M. A. Halim, S. B. Donaev, and S. Wang, "Fabrication of iron pyrite thin films and photovoltaic devices by sulfurization in electrodeposition method," Nanomaterials, 11 (2021) 2844. https://doi.org/10.3390/nano11112844.

[2] P. L. Gareso and E. Juarlin, "Optical and structural characterization of ZnO/TiO2 bilayer thin films grown by sol-gel spin coating," in Journal of Physics: Conference Series, 979 (2018) 012060. https://doi.org/10.1088/1742-6596/979/1/012060.

[3] Jasim, S., Kzar, H. H., Sivaraman, R., Jweeg, M. J., Zaidi, M., Alkadir, O. K. A., Safaa Fahim, F., Obaid Aldulaim, A. K., Kianfar, E. Engineered Nanomaterials, Plants, Plant Toxicity and Biotransformation: A review. Egyptian Journal of Chemistry, 65 (2022)151-164. doi: 10.21608/ejchem.2022.131166.5775

[4] R. Hussin, N. S. Zulkiflee, K. Zakiah, A. A. Rahmahwati, Z. Harun, and M. N. M. Hatta, "Photocatalytic activity of bilayer TiO2/ZnO and ZnO TiO2 thin films," in Materials Science Forum, 1010 (2020) 411-417. https://doi.org/10.4028/www.scientific.net/msf.1010.411.

[5] S. Sakka, "Handbook of Advanced Ceramics: Chapter 11.1. 2. Sol–Gel Process and Applications," Elsevier Inc. Chapters, 2013. https://doi.org/10.1016/b978-0-12-385469-8.00048-4.

[6] El-Shehry, M.F., El-Hag, F.A.A. & Ewies, E.F. Synthesis and Antimicrobial Study of New Fused Thiazolo[3,2-b]triazine, Triazolo[4,3-b]triazine, and 1,2,4-Triazinone Derivatives. Russ J Org Chem 56 (2020) 129–136. https://doi.org/10.1134/S1070428020010200

[7] P. Innocenzi, "The precursors of the sol-gel process," in The Sol-to-Gel Transition, (2019) 7-19. https://doi.org/10.1007/978-3-030-20030-5_2.

[8] J. Livage, "Sol-gel processes," Current Opinion in Solid State and Materials Science, 2 (1997) 132-138. https://doi.org/10.1016/s1359-0286(97)80057-5.

[9] D. Ganguli, "Sol-gel processing of materials for electronic and related applications," Bulletin of Materials Science, 15 (1992) 421-430. http://cgcri.csircentral.net/id/eprint/2331.

[10] Z. C. Wang, J. Miao, M. Yang, R. H. Zhao, Y. Wu, X. G. Xu, and Y. Jiang, "Ultra-high photocurrent response in a chromium oxide thin film under visible light illumination," Journal of Alloys and Compounds, 723(2017) 311-316. https://doi.org/10.1016/j.jallcom.2017.06.109.

[11] G. Szitasi, F. Korsos, D. Selmeczi, O. Takacs, F. Novinics, P. Tutto, A. Findlay, and M. Wilson, "Integrated electrical and optical characterization of large area thin film photovoltaic materials," in 2012 38th IEEE Photovoltaic Specialists Conference, (2012) 474-478. https://doi.org/10.1109/pvsc.2012.6317660.

[12] A. Cachard, "Physico-Chemical analysis of thin films," in Physics of Nonmetallic Thin Films, Boston, MA: Springer US, (1976)141-161. https://doi.org/10.1007/978-1-4684-0847-86.

[13] K. C. Gödel and U. Steiner, "Thin film synthesis of SbSI micro-crystals for self-powered photodetectors with rapid time response," Nano-scale, 8 (2016)15920-15925. https://doi.org/10.1039/C6NR04759A.

[14] J.-H. Kim, H. Kim, K. Cho, and S. Kim, "Time-dependent photocurrent of a CdTe nanoparticle film under the above-gap illumination," Solid state communications, 136 (2005) 220-223, 2005. https://doi.org/10.1016/j.ssc.2005.07.020.

[15] J. Lee and J. Kong, "Dark currents in bulk heterojunction devices for imaging applications: The effect of a cathode interfacial layer," Current Applied Physics, 14 (2014) 649-652, 2014. https://doi.org/10.1016/j.cap.2014.02.007.

[16] J. Kim et al., "Enhanced Performance of I2☐Free Solid☐State Dye☐Sensitized Solar Cells with Conductive Polymer up to 6.8%," Advanced Functional Materials, 21(2011) 4633-4639. https://doi.org/10.1002/adfm.201101520.

[17] S. R. Jadkar et al., "Thin Film Materials and Devices," ES Mater. Manuf., 10 (2020) 1-4. https://doi.org/10.30919/esmm5f970.

[18] Y. Jiang et al., "Optical and interfacial layer properties of SiO2 films deposited on different substrates, "AppliedOptics, 53 (2014) A83-A87. https://doi.org/10.1364/ao.53.000a83.

[19] A. A. Auda, H. A. Banimuslem, and B. Y. Kadim, "Photoresistance Characteristics of ZnO: TiO2 Nano-Heterostructure Synthesized by Sol–Gel Method," Journal of Nanostructures, In Press, April 13, 2023.

[20] E. D. Jones et al., Thin-film structures for photovoltaics, Warrendale, PA (United States): Materials Research Society, 1998.

[21] K. Wasapinyokul, W. I. Milne, and D. P. Chu, "Photoresponse and saturation behaviour of organic thin film transistors," Journal of Applied Physics, 105(2009) 2009. https://doi.org/10.1063/1.3068359.

[22] N. Naseri, M. Yousefi, and A. Z. Moshfegh, "A comparative study on the photoelectrochemical activity of ZnO/ TiO2 and TiO2/ZnO nanolayer systems under visible irradiation," Solar energy, 85 (2011) 1972-1978. https://doi.org/10.1016/j.solener.2011.05.002.

[23] J. Wu, H. Li, Y. Liu, and C. Xie, "Photoconductivity and trap-related decay in porous TiO2/ZnO nanocomposites," Journal of Applied Physics, 110 (2011) 2011. https://doi.org/10.1063/1.3662954.

[24] B. K. Barnes and K. S. Das, "Resistance switching and memristive hysteresis in visible-light-activated adsorbed ZnO thin films," Scientific Reports, 8 (2018) 2184, 2018. https://doi.org/10.1038/s41598-018-20598-5.

[25] M. Bauza et al., "Light-induced metastability in thin nanocrystalline silicon films," Philosophical Magazine, 89 (2009) 2531-2539, 2009.

[26] A. Sáenz-Trevizo et al., "Optical band gap estimation of ZnO nanorods," Materials Research, 19 (2016) 33-38. https://doi.org/10.1590/1980-5373-mr-2015-0612.

[27] R. Koole et al., "Size effects on semiconductor nanoparticles," in Nanoparticles: Workhorses of Nanoscience, (2014) 13-51.

[28] Y. Liao et al., "Characterization of photoelectric properties and composition effect of TiO2/ZnO/Fe2O3 composite by combinatorial methodology," Journal of Combinatorial Chemistry, 12 (2010) 883-889. https//doi.org/10.1021/cc100121d.

[29] T. Georgakopoulos et al., "On the transient photoconductivity behaviour of sol–gel TiO2/ZnO composite thin films," Journal of Non-Crystalline Solids, 410 (2015) 135-141, 2015. https://doi.org/10.1016/j.jnoncrysol.2014.11.034.